Electronic structure and magnetism of europium chalcogenides in comparison with gadolinium nitride

2006 J. Phys.: Condens. Matter 18 11333

(http://iopscience.iop.org/0953-8984/18/49/024)

INSTITUTE OF PHYSICS PUBLISHING JOURNAL OF PHYSICS: CONDENSED MATTER

J. Phys.: Condens. Matter **18** (2006) 11333–11345 doi:10.1088/0953-8984/18/49/024

Electronic structure and magnetism of europium chalcogenides in comparison with gadolinium nitride

Paul Larson and Walter R L Lambrecht

Department of Physics, Case Western Reserve University, 10900 Euclid Avenue, Cleveland, OH 44106-7079, USA

Received 21 June 2006, in final form 28 August 2006
Published 23 November 2006
Online at stacks.iop.org/JPhysCM/18/11333

Abstract

Electronic structure calculations were carried out for the europium chalcogenides (EuO, EuS, EuSe, EuTe) using the 'LSDA + U' approach, in which orbital-dependent Coulomb and exchange effects are added to the local spin density approximation (LSDA) for the f electrons. The usual LSDA gap underestimate is also corrected by adding U_d terms, which shift up the empty d states. While both GdN and EuO are found to be magnetic semiconductors, there are significant differences in the electronic structure, in particular in the location of the filled f bands. The origin of these differences and their effect on various other aspects of the band structure are discussed. The exchange coupling between magnetic moments is studied by mapping the energy differences of different magnetic configurations to a Heisenberg Hamiltonian with first- and second-nearest-neighbour interactions. The exchange interactions are in fair agreement with experimental values and explain the trends in magnetic properties.

(Some figures in this article are in colour only in the electronic version)

1. Introduction

The emergence of the field of spintronics [1, 2] has led to a renewed interest in ferromagnetic semiconductors such as EuO and GdN, whose magnetism arises from the partially filled and highly localized 4f states. Unlike most ferromagnetic semiconductors studied currently, these are bulk as opposed to dilute magnetic semiconductors. The best known of this class of rare-earth (RE) based magnetic semiconductors is EuO, which has a moment of 7 μ_B and a bandgap of 1.12 eV [3, 4]. This system has been studied extensively both experimentally [5–9] and theoretically [4, 10–13]. EuO has many similarities with GdN, another rare-earth material, which also forms in the rock-salt structure and has also been found to be a ferromagnet with a Curie temperature (T_c) of 58 K [14–16] compared to 69 K for EuO [4–6]. Eu in EuO is divalent and Gd in GdN is trivalent so that the 4f orbitals are half-filled in both cases. The valence bands are made up of 2p states of O and N, respectively. One would thus expect similar properties

for these two materials. It has been suggested that the mechanism for strong ferromagnetism in GdN is different from that in EuO [17].

The semiconducting or semimetallic nature of GdN is still under discussion. Pure stoichiometric samples (free of oxygen impurities and nitrogen vacancies) are difficult to produce [16], leading to high carrier concentrations, which make it difficult to distinguish between a heavily doped n-type semiconductor and a semimetal. On the other hand, the temperature dependence of the resistivity [18] as well as the existence of an optical absorption edge of about 1 eV [15] clearly suggest a semiconductor, at least above the Curie temperature. Recent measurements have suggested that GdN goes through a semiconductor to metal transition when the temperature is lowered below the Curie temperature T_c [19], but other measurements conclude that it is merely a red-shift of the bandgap, which does not go all the way to zero [20]. On the theoretical side, the challenge is to deal with the strongly correlated properties of f electrons as well as the usual local density approximation bandgap problem. Arguments for both a narrow-gap semiconductor [21, 22] and a very weak semimetal [24] have been made in the literature. In either case, it may be a useful material for (low-temperature) spin-injection into semiconductors because of its relatively high resistivity making it compatible with semiconductors, and its complete spin-polarization of the conduction band in the ferromagnetic state [25].

In this paper, we present results obtained using the LSDA + U approach, which allows us to handle both of the above mentioned challenges of f orbitals and calculated bandgaps as explained in section 2. We present results for the band structures of the Eu chalcogenides with particular emphasis on EuO, including a comparison with GdN. Our results on GdN were presented more fully in a paper on the entire series of Gd pnictides [22]. Although the LSDA + U approach has a certain semi-empirical character in the choice of the Coulomb parameters, it is more flexible and simpler than the alternative self-interaction correction (SIC) approach, which has often been applied to rare-earth compounds, notably in a study on the related rare-earth nitrides [23].

We also consider the magnetic properties. The heavier members of the family belonging to GdN and EuO become antiferromagnetic (AFM), including GdP, GdAs, GdSb, and GdBi [17, 22, 26–28] as well as EuSe and EuTe [4, 11, 29–33]. EuS remains ferromagnetic with a lower T_c and a second-neighbour coupling constant (J_2) which becomes negative but smaller than the nearest-neighbour coupling constant (J_1) [4, 34, 35]. The AFM ordering for the heavier members of both series occurs along the {111} direction [4, 26, 27, 29] with the exception of EuSe, which has a spiral type of magnetic ordering [36], indicative of a competition between ferro- and antiferromagnetic interactions.

The paper is organized as follows. In section 2 we briefly describe the computational approach. In section 3.1 we give the equilibrium lattice constants obtained from our calculations in comparison with experiment. In section 3.2 we discuss the band structure of EuO in comparison with GdN. In section 3.3 we present the band structure of the other chalcogenides and summarize the trends. In section 3.4 we present our results for the magnetic exchange interactions. Finally, we summarize the main conclusions in section 4.

2. Computational method

Electronic structure calculations were carried out within the local spin density approximation (LSDA) to density functional theory (DFT) [37] using a full-potential linearized muffin-tin orbital (FP-LMTO) program [38] employing the exchange–correlation parameterization of von Barth and Hedin [39] complemented with Hubbard-U corrections for the f electrons. This method uses an optimized basis set consisting of muffin-tin orbitals with smoothed Hankel

functions as envelope functions. The smoothing radii and κ values (Hankel function decay parameter) were carefully adjusted to optimize an efficient basis set with one s, p, and d function on the N or O site and two s and p and a single d and f function on each Gd or Eu site. The smooth interstitial quantities are calculated using a fast Fourier transform mesh and the Brillouin zone integrations were carried out using the tetrahedron method [40, 41] with a well converged k-mesh based on a division of the reciprocal unit cell in $6 \times 6 \times 6$ divisions.

The partially filled and strongly correlated localized f orbitals were treated using the LSDA + U method [42–44], where the double-counting terms are subtracted in the fully localized limit (FLL), which best describes the localized nature of the 4f orbitals. The present implementation in the van Schilfgaarde FP-LMTO *lmf* program follows the rotationally invariant formulation of Liechtenstein *et al* [43] written in terms of the density matrix $n^{\sigma}_{mm'}$ and Coulomb matrix elements $\langle mm''|V_{ee}|m'm'''\rangle$. Essentially, the Coulomb and exchange interactions in the Hartree–Fock approximation for the localized f states are added to the local spin density total energy functional and a double-counting correction is subtracted. The functional thereby depends not only on the total spin density but also the density matrix of the localized orbitals. The minimization problem then leads to an additional orbital dependent potential $V^{\sigma}_{mm'}$. In general, it includes non-spherical terms, described in terms of the Slater–Coulomb integrals F^k with $k = 0, 2, 4, 6$. However, for the half-filled case, only a spherical average exchange interaction J enters the problem. As is customary, it is assumed that the spherically averaged Coulomb interaction parameter U is a screened F^0, whereas screening is negligible for the F^2–F^6, which can therefore be taken from atomic calculations. The average J is given by

$$J = (286F^2 + 195F^4 + 250F^6)/6435. \tag{1}$$

The F^k parameters are taken from Hartree–Fock calculations for the elements as tabulated by Mann [45]. In order to obtain the screened U value, we take a semi-empirical approach. The splitting of the occupied and empty f levels is given by $(U - J)$ and is taken from photoemission data for the Gd pnictides [22, 28]. It is found to be nearly independent of the group-V element and thus the same value was used for GdN and the other Gd pnictides, leading to good agreement for the position of the occupied 4f levels as measured by photoemission [19, 22]. For EuO, we scale the value of U in proportion of the Eu to Gd atomic F^0 values. This assumes the same screening applies in both cases. The values used for Eu are $U_{\mathrm{f}} = 7.397$ eV and $J_{\mathrm{f}} = 1.109$ eV, while the values for Gd are $U_{\mathrm{f}} = 8.0$ eV and $J_{\mathrm{f}} = 1.222$ eV.

In the present case of a half-filled shell, Hund's rules predict a maximum $S = 7/2$ and $L = 0$. The f states are thus spherically symmetric. In order to avoid numerical instabilities, we impose symmetrization of the density matrix according to the crystal's cubic symmetry. The density matrix is made self-consistent to allow for hybridization with the other states in the system. In fact it stays close to the initial starting point, in which it is diagonal and has states for one spin occupied and states for the other spin empty.

Besides the problem of strongly correlated f electrons, we need to deal with the usual LSDA bandgap problem. The best approach to date to deal with this problem is the GW approach [46–50], in which the quasiparticle self-energy, schematically given as the product of the one-electron Green's function G and the screened Coulomb interaction W, replaces the exchange and correlation potential of the Kohn–Sham equations. In the present case, the conduction band consists primarily of the Gd or Eu d states. Thus a shift of the d states will mimic the GW self-energy effect. This can be implemented by means of the same LSDA + U approach, since the additional potential (in the spherically averaged case) is

$$V^{\sigma}_{mm'} = -(U - J)(n^{\sigma}_{mm'} - \tfrac{1}{2}\delta_{mm'}), \tag{2}$$

and this leads to an upward shift by $(U - J)/2$ for empty states ($n^{\sigma}_{mm'} = 0$). Thus we can easily

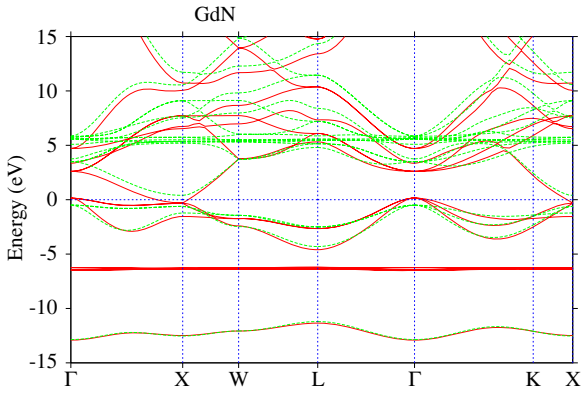

Figure 1. Electronic band structure of GdN in LSDA + U with $U_f = 8$ eV, $J_f = 1.222$ eV, $U_d = 3.4$ eV and $J_d = 0$ eV. Solid (red) lines are for the majority and dashed (green) lines for the minority spin state.

Table 1. Lattice constants of europium chalcogenides (in Å).

	Theory	Experiment
EuO	5.14	5.141
EuS	5.97	5.968
EuSe	6.20	6.195
EuTe	6.60	6.598

apply a shift to the d states. For simplicity we treat $(U_d - J_d)$ as an empirical parameter. It was determined in the case of GdN by adjusting the average of the spin-up and spin-down direct gaps at the X-point of the Brillouin zone to the corresponding onset of optical absorption at 0.98 eV [21]. The reason why we average the gaps of both spins is that this optical absorption measurement was carried out at room temperature, i.e. in the paramagnetic state [51]. As was shown in [22] this leads to an almost negligible indirect gap in the ferromagnetic state for the majority spin, consistent with the significant red-shift observed by Granville *et al* [20] and possibly the semiconductor to metal transition observed by Leuenberger *et al* [19]. The same value of $(U_d - J_d) = 3.4$ eV is applied to Eu d states and will be seen to lead to good agreement for the bandgaps.

3. Results

3.1. Lattice constants

All the Eu chalcogenides and Gd pnictides form in the rock-salt crystal structure. Their lattice constants were determined so as to minimize the total energy and are found to lie very close to the experimental values. The results are summarized in table 1. The same excellent degree of comparison was obtained for Gd pnictides [22].

3.2. Band structure of EuO and GdN

Although our results for GdN were presented previously [22], in order to keep the present paper self-contained we first show the band structure of GdN in figure 1 for comparison with that of EuO. We notice that the majority spin 4f states lie well below the N 2p valence band, in the

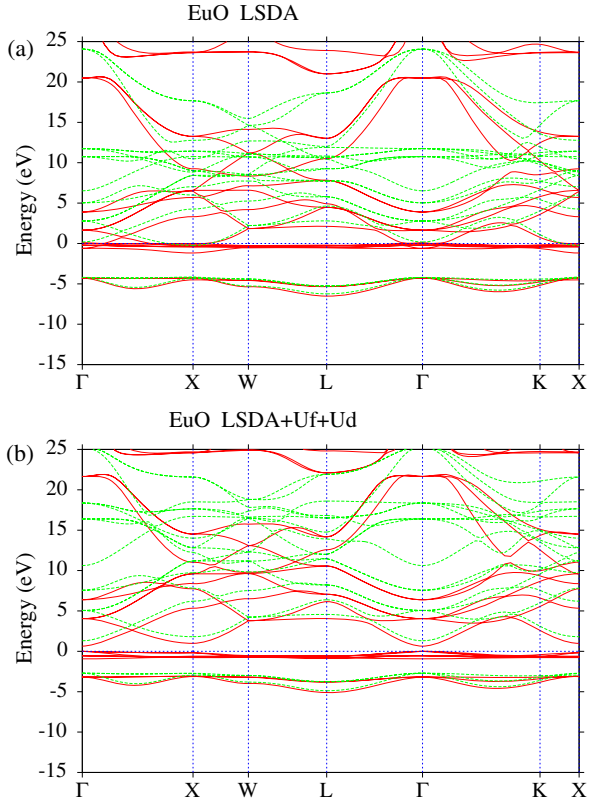

Figure 2. Electronic structure of EuO for (a) LSDA and and (b) LSDA + U with $U_f = 7.397$ eV, $J_f = 1.109$ eV, $U_d = 3.4$ eV and $J_d = 0$ eV. Colour coding the same as in figure 1.

gap between N 2p and N 2s states. In LSDA they would overlap the N 2p bands [22]. The minority spin states lie about equally high above the Fermi level but are somewhat broader due to hybridization with the conduction band states. The valence band maximum is of N 2p character and the conduction band minimum consists of Gd 5d states. The Gd 6s band is almost degenerate with the lowest triply degenerate Γ_{15c} d state for the majority spin. The non-degenerate minority spin Γ_{1c} Gd 6s state can be recognized just above it. The minimum gap is indirect along Γ–X and is seen to be significantly smaller for majority than minority spin because of the inversion of the spin states in the conduction and valence bands. In fact, the minimum gap is almost zero, whereas the average gap, which would be applicable above T_c, is 0.69 eV.

The band structure of EuO is shown in figure 2 both for LSDA and for LSDA + U as calculated with the parameters specified above. Significant differences with GdN are apparent. In LSDA as well as in LSDA + U, the occupied f states lie right at the Fermi level, above the O 2p states. The Eu 5d states still form the bottom of the conduction band at X, but at Γ the Eu 6s state is now distinctly below the Γ_{15c}. The unoccupied f states mostly lie around 12 eV in LSDA and around 17 eV in LSDA + U. One may recognize the a_{1u} f state of minority spin to be the non-degenerate state at Γ at 7 eV in LSDA and 11 eV in LSDA + U. The next two triply degenerate states at Γ are also f-like. These bands show considerable dispersion and hybridization with the conduction band at other k-points.

In GdN the shift of the occupied and unoccupied f states is almost uniformly away from the Fermi level, each being shifted by approximately $(U - J)/2$. However, in EuO the unoccupied state moves up by about 5 eV (close to $U - J = 6$ eV) with respect to E_F while the position of the occupied state moves down less than 1 eV. The origin for the difference in the shift between GdN and EuO lies in the relative position of the 4f band with respect to the 2p valence band. In GdN, LSDA calculations place the Gd 4f states in the middle of the N 2p band. The spin splitting of these N bands near Γ is 1.2 eV due to the close proximity of the occupied Gd 4f states. The U_f and J_f parameters shift the occupied f states from -3.6 to -6.7 eV, several eV below the N 2p band. The reduced hybridization between the N 2p and Gd 4f states reduces the spin splitting of the top of the valence band at Γ to 0.5 eV.

The situation in EuO is exactly the opposite. When adding the U_f shifts, the occupied Eu 4f states move closer to the O 2p states and hence increase the hybridization instead of reducing it. This is manifested in the fact that the spin splitting of the O 2p states increases from less than 0.1 eV to about 0.4 eV when the U_f terms are switched on. The result is that when the majority-spin Eu 4f states try to move down they become repelled by the O 2p states below by the increased hybridization. Thus they can hardly move down. Since the Eu 4f levels determine the valence band maximum, they stay at the Fermi level, and instead of seeing the 4f moving down, we rather see the O 2p levels move up towards it if we keep the Fermi level as reference energy. The minority spin Eu 4f states, on the other hand, move up by the U_f effects and thus do not encounter this problem. They become less hybridized with O 2p and hence, being more purely Eu f character, feel a stronger upward interaction from the Eu d bands below them, which pushes them up further than the expected $(U - J)/2$. One may understand the reason for this difference between GdN and EuO in two ways. One is that O 2p states lie deeper than N 2p states on an absolute scale. Alternatively, the f states experience a less repulsive electrostatic environment when surrounded by a group-V element N than by a group-VI element O. Thus, the stronger ionicity of a II–VI compound can be viewed as part of the reason why the occupied f states lie above the O 2p levels in EuO but below or close to the N 2p levels in GdN.

Having discussed the effects of the position of the 4f states relative to the bands, we now turn to a discussion of the bandgap. If we include LSDA + U corrections only for the Eu 4f orbitals but not for the Eu 5d orbitals (not shown), we find a narrow indirect gap of 0.18 eV between the Eu 4f band valence band maximum at Γ and the Eu 5d conduction band minimum at X. Addition of the 5d shift (as in figure 2(b)) leads to a switch of the conduction band minimum to the Γ point Eu 6s state. The lowest bandgap then becomes direct at Γ with a value of 0.64 eV for majority spin states. This is smaller than the experimental value of 1.12 eV [4], but one must remember, as in GdN [19, 21], that the bandgap was measured above T_c in the paramagnetic range [4]. The average of the spin-up and spin-down bands may be considered to approximate the position of the band in the paramagnetic state. When this is done, the bandgap is 0.97 eV, much closer to the experimental value of 1.12 eV [4, 11]. Direct evidence for the spin splitting of the conduction band was presented by Steeneken *et al* [7], using spin-dependent x-ray absorption measurements. Our calculated spin splitting of the conduction band of 0.66 eV is close to the experimental value of 0.6 eV. This also agrees with the redshift of the absorption coefficient from the paramagnetic to the ferromagnetic state, which is about 0.3 eV [9], corresponding to half the spin splitting.

The value of U_d for Eu could differ slightly from that for Gd, and, in addition, one might also expect a GW self-energy shift of the Eu 6s state, which has now become the conduction band minimum. Thus whether the bandgap is really direct or indirect cannot be firmly concluded from our calculations. The band structure looks similar to other recent LSDA+U calculations [4], but the position of the 4f orbitals and the size of the bandgaps differ

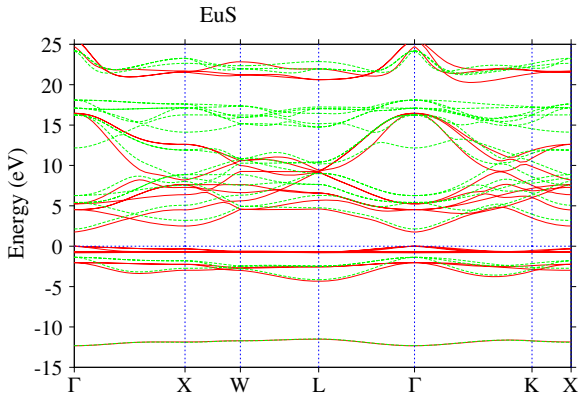

Figure 3. Band structure of EuS in LSDA + U_f + U_d. Colour coding the same as in figure 1.

slightly due to different values of U and J. The early augmented plane waveband structure calculation of Cho *et al* [13] gave an indirect bandgap with conduction band minimum at X but used essentially Slater's exchange approximation, which should be less accurate than the present LSDA + U approach. Since the f bands are quite flat, it is quite difficult to distinguish experimentally between a direct or indirect bandgap and to locate the k-point position of the valence band maximum. UV reflectivity or spectroscopic ellipsometry for higher energy interband transitions between the anion p valence band and the conduction band may be useful to determine the actual location of the conduction band minimum.

Another noteworthy difference between GdN and EuO in their band structures is the sign of the spin splittings of the anion p bands. In EuO, these minority spin states lie above the majority ones, whereas in GdN they are reversed. This is again due to the hybridization with the 4f states. In GdN, the $4f_\downarrow$ (majority) lie below the N 2p and hence the N $2p_\downarrow$ are moved up, while the $4f_\uparrow$ lie above the N $2p_\uparrow$, which moves them down. In EuO, both $4f_\uparrow$ and $4f_\downarrow$ lie above the O 2p, thus pushing the O 2p states down for both spins, but the majority ($\downarrow$) states feel a stronger interaction because the $4f_\downarrow$ states are closer in energy to them. The Gd and Eu 5d states and 6s states, on the other hand, all experience the normal spin ordering, minority spin above majority spin. This means that for Eu compounds optical transitions between the O 2p bands and Eu 5d or Eu 6s bands will show little spin polarization, because the shifts in occupied and empty states are in the same direction and are subtracted in the transition. For GdN, however, the shifts in the occupied and empty states will add because they are in opposite directions.

3.3. Band structure of other Eu chalcogenides

In figures 3–5 we present LSDA + U_f + U_d results for the band structures of EuS, EuSe and EuTe, respectively. They are quite similar to those of EuO. The anion derived valence bands move closer to the f states as expected. By EuSe, the gap between Se p bands and Eu f bands has closed, and in EuTe the f bands have moved to the middle of the Te p valence bands. Thus, there is progressively more hybridization between the anion p and Eu f states. In all cases we find the conduction band minimum corresponds to the Γ_{1c} Eu 6s state. However, this is related to the fact that we have applied a gap shift for the d states and not for the 6s states. Nevertheless, even if we do not include a U_d shift, the 6s and 5d states are very close in energy and thus the question of whether the gaps are direct or indirect remains unclear.

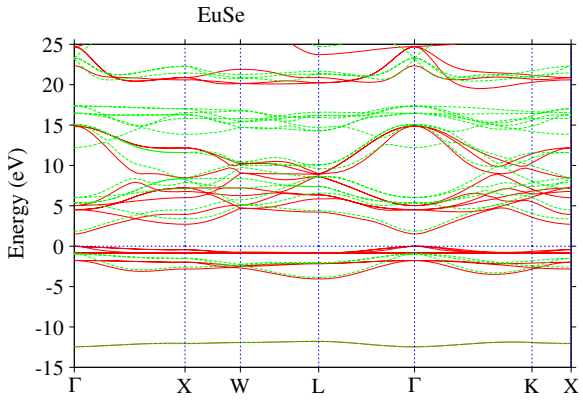

Figure 4. Band structure of EuSe in LSDA + U_f + U_d. Colour coding the same as in figure 1.

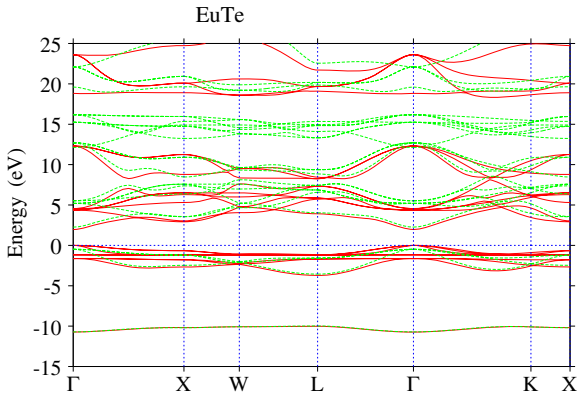

Figure 5. Band structure of EuTe in LSDA + U_f + U_d. Colour coding the same as in figure 1.

An overview of the various bandgaps in comparison with previous work and in comparison between the two materials is given in table 2. While the filled Eu 4f states agree well with Ghosh *et al* [4], the unoccupied states lie much lower in energy, most likely a result of using smaller values of U_f (5.0 versus 7.4 eV) and different computational methods.

3.4. Magnetism

The magnetic properties of EuO and GdN are surprisingly similar. Note for example the similar values of T_c and the magnetic moments [17]. The different relative position of the 4f with respect to the anion p bands would lead one to expect far weaker indirect exchange interactions for GdN than for EuO [17]. Kasuya and Li [17] attempt to make sense of this by explaining the nearest-neighbour exchange interaction in Eu chalcogenides. This is dominated by an indirect interaction arising from the virtual excitation of a 4f to a 5d state, which then overlaps with the neighbouring Eu and leads to an f–f interaction via the f–d exchange. The f–d exchange J_{df} essentially measures the spin splitting of the d bands induced by their intra-atomic interaction with the spin-polarized f state. One may view the effect as arising from the hopping of the f electron to a neighbouring site d orbital, where it is subject to a spin exchange interaction J_{df}. In perturbation theory, it means that the d orbital gets mixed into the f band in an amount

Table 2. Bandgap parameters in GdN and Eu chalcogenides.

	U_d	EuO	EuS	EuSe	EuTe	GdN
Majority spin Γ–Γ gap	No	0.68	1.68	1.44	1.94	2.49
Majority spin Γ–Γ gap	Yes	0.64	1.75	1.50	1.96	3.18
Paramagnetic Γ–Γ gap	No	1.02	1.87	1.62	2.09	3.18
Paramagnetic Γ–Γ gap	Yes	0.97	1.94	1.88	2.11	3.63
Majority spin Γ–X gap	No	0.15	1.54	1.76	2.01	−0.42
Majority spin Γ–X gap	Yes	0.98	2.49	2.71	2.92	0.12
Paramagnetic Γ–X gap	No	0.57	1.90	2.09	2.35	0.15
Paramagnetic Γ–X gap	Yes	1.31	2.84	3.05	3.22	0.69
Majority spin X–X gap	No	0.32	1.83	2.13	2.57	−0.04
Majority spin X–X gap	Yes	1.17	2.82	3.14	3.58	0.57
Paramagnetic X–X gap	No	0.75	2.19	2.48	2.91	0.42
Paramagnetic X–X gap	Yes	1.58	3.17	3.48	3.88	0.99
Paramagnetic gap (experiment)[a]		1.12	1.65	1.80	2.00	0.98[b]
Occupied 4f relative to E_F	Yes	−0.64	−0.71	−0.83	−1.14	−6.70
Occupied 4f relative to E_F [a]		−1.0	−1.5	−2.0	−2.5	−6.5
Empty 4f relative to E_F	Yes	17.4	16.7	16.9	15.7	7.80
Empty 4f relative to E_F [a]		7.5	5.5	5.0	3.0	5.0

[a] From Dimmock [33] for Eu chalcogenides and Hulliger *et al* [14] for GdN.
[b] GdN paramagnetic gap measured at X.

$t_{df}/(\epsilon_d - \epsilon_f)$, where t_{df} is the hopping integral. The corresponding contribution to the exchange interaction between nearest-neighbour f sites (in third-order perturbation) is

$$J_1^{\text{indirect}} \propto J_{df}\frac{t_{df}^2}{(\epsilon_d - \epsilon_f)^2}. \tag{3}$$

Obviously, since the $(\epsilon_d - \epsilon_f)$ splitting is much larger in Gd compounds than Eu compounds, one would expect a smaller J_1. Kasuya and Li [17] proposed that a fourth-order process involving the N 2p states as well as the Gd d states gives rise to a comparably strong J_1 in Gd but barely affects the Eu J_1.

It is clearly of interest to see whether the comparable exchange interactions J_1 in Gd and Eu compounds can be reproduced by our first-principle total energy calculations. Our approach is to fit the total energy differences of specified magnetic alignment configurations to a Heisenberg model in order to extract the nearest-neighbour and next-nearest-neighbour coupling constants. Following Yosida [52], we write the Heisenberg Hamiltonian as

$$H = -2\sum_{i>j} J_{ij}\mathbf{S_i}\cdot\mathbf{S_j} \tag{4}$$

where $S = \frac{7}{2}$ is the total moment ($L = 0$ for half-filled shells). Using the ferromagnetic (FM) and antiferromagnetic (AFM) orderings [53] AFM_I where spins alternate by layer along {001} and AFM_{II} where spins alternate by layer along {111}, we can extract the first- and second-nearest-neighbour coupling constants J_1 and J_2. A third configuration AFM_{III}, where spins alternate every two layers along {001}, provides a check on the adequacy of the Heisenberg Hamiltonian. Previous calculations for GdN [24, 54] have found the third-nearest coupling constant, J_3 to be very small, so we will not consider it here. Positive coupling constants correspond to ferromagnetic interactions while negative values correspond to antiferromagnetic interactions. The energies for the four states considered here can be written as

$$E_{FM} = E_0 + S(S+1)(-12J_1 - 6J_2) \tag{5a}$$

$$E_{AFM_I} = E_0 + S(S+1)(4J_1 - 6J_2) \tag{5b}$$

Table 3. Energy of antiferromagnetic configurations relative to the ferromagnetic one for Eu chalcogenides and GdN (in meV/unit cell).

	EuO	EuS	EuSe	EuTe	GdN
$[001]_1$	15.61	5.02	2.40	−0.06	15.09
$[111]_1$	15.22	−0.37	−3.69	−6.39	6.07
$[001]_2$	9.19	1.35	−0.48	−2.07	10.20
$[001]_2$ [a]	8.97	1.13	−0.63	−2.15	5.8

[a] As obtained from the model with J_1 and J_2 only.

Table 4. Exchange parameters in Eu chalcogenides and GdN in K.

		EuO	EuS	EuSe	EuTe	GdN
Our results	J_1	0.72	0.23	0.11	−0.003	0.695
	J_2	0.22	−0.25	−0.34	−0.39	−0.32
Thermodynamic data	J_1	0.665	0.19	0.125	0.015	0.64
	J_2	−0.06	−0.08	−0.12	−0.155	0
Neutron scattering	J_1	0.606	0.236			
	J_2	0.119	−0.118			

[a] Extracted from paramagnetic temperature and Curie or Néel temperature in mean field theory, from [36] for Eu compounds and [16] for GdN.
[b] From inelastic neutron scattering measurements of the spin-wave excitations, [55].

$$E_{\mathrm{AFM_{II}}} = E_0 + S(S+1)(6J_2) \tag{5c}$$

$$E_{\mathrm{AFM_{III}}} = E_0 + S(S+1)(-4J_1 - 2J_2). \tag{5d}$$

The energies of the various AFM configurations relative to the FM one are given in table 3. The exchange coupling constants obtained for all Eu compounds and for GdN are given in table 4. The last row in table 3 shows the values obtained from equation (5*d*) and with the J_1 and J_2 from table 4. The agreement with the result directly obtained from first principles is quite good in most cases and clearly accounts for the correct trend. The exchange parameters are compared with the values obtained from thermodynamic data by Kasuya *et al* [16, 36] and with the neutron scattering results of Passell *et al* [55]. While our values seem to be slight overestimates, they agree on the key features. First, we find a comparable J_1 for EuO and GdN. Second, we find a decreasing trend of J_1 as we go from O to Te. Third, in agreement with Passell *et al* [55] we find a change of sign for J_2 for EuSe compared to EuO. We note that the measurements of Passell *et al* [55] give the most direct result on the exchange interactions within the Heisenberg Hamiltonian, because they do not require a mean-field approximation to adjust to the critical temperatures. Kasuya *et al* [36] give negative J_2 values for all Eu chalcogenides. In agreement with his results, we see a trend of increasingly more negative values of J_2 as we go from Se to Te, although the changes are less strong than for J_1. For GdN we note that Li *et al* [16] did not include a J_2 in their analysis.

In disagreement with experiment, we already find EuS to have a lower energy for the antiferromagnetic $\mathrm{AFM_{II}}$ configuration, although the energy difference from the FM state is quite small. It means that J_1 and J_2 are close in absolute value but with opposite sign because the energy difference between $\mathrm{AFM_{II}}$ and FM state is proportional to $J_1 + J_2$. In the results of Kasuya *et al* [36] this situation occurs for EuSe instead of EuS. It is responsible for the complex spin arrangement found in EuSe. Thus our calculations seem to favour antiferromagnetism too strongly compared to experiment. While this may be a computational error, we note that experimentally there may be a contribution to the ferromagnetic interaction arising from carrier mediated effects.

Table 5. Calculated (from mean field theory according to equation (7) with first-principles exchange interactions from table 4) and experimental values for magnetic temperatures.

		EuO	EuS	EuSe	EuTe	GdN
Calc.	θ_P	104	13	−7	−25	67
	T_N		16	21	24	
Expt	θ_P (K)	80	19	8	−6	81
	T_N (K)			5	10	
	T_c (K)	69	16			58

[a] From [36] and [55] for Eu compounds and [16] for GdN.

Finally, we can use our computed exchange interactions to calculate magnetic temperatures and compare them to experimental data. The Néel temperature T_N for the AFM_{II} configuration and the paramagnetic Curie–Weiss temperature θ_P in mean field theory are given by

$$k_B T_N = -4S(S+1)J_2, \tag{6}$$

$$k_B \theta_P = 4S(S+1)(2J_1 + J_2), \tag{7}$$

while for the ferromagnetic case in mean field theory the Curie temperature equals the Curie–Weiss temperature $T_c = \theta_P$. The results are shown in table 5. As is to be expected from mean field theory, the Néel temperatures and Curie temperatures are strongly overestimated. Nevertheless, the trend of decreasing θ_P from O to Te agrees qualitatively with experiment. In EuS, both theory and experiment find T_N (or T_c) to be close to θ_P.

4. Conclusions

The electronic structure and magnetic properties of europium chalcogenides EuO, EuS, EuSe, and EuTe were studied and compared to those of GdN using the LSDA + U_f + U_d approach. The crucial difference between EuO and GdN is that the occupied majority spin 4f levels lie above the O 2p valence band in EuO but below the N 2p valence band in GdN. In the other chalcogenides, the Eu $4f_\downarrow$ band approaches the anion p valence band and starts merging with it for EuSe and EuTe. The effect of the U_f in LSDA + U is rather different in GdN from the Eu compounds. In GdN the occupied (majority spin) and empty (minority spin) 4f bands are about equally pushed away from the Fermi level by $(U - J)/2$, whereas in the Eu compounds the occupied 4f levels move down only slightly toward the anion p band because they are being repelled by their mutual hybridization, while the empty 4f levels take the majority of the $(U - J)$ shift. The occupied 4f levels are the highest occupied states and thus form the actual valence band maximum, except for EuTe, where the 4f band has moved to the middle of the anion p valence band. Another noteworthy difference is that in GdN the 5d conduction band at X is definitely lower than the Gd 6s conduction band at Γ. In Eu compounds the 6s level at Γ lies slightly deeper with respect to the 5d level at X, so when a U_d shift is included the conduction band minimum switches to the Γ_{1c} Eu 6s state. It is not clear, however, whether further corrections to LSDA would also push the 6s state upward and restore an indirect gap. Experimentally, it is difficult to determine whether the gap is direct or indirect because the 4f valence band is almost dispersionless. The minimum optical absorption can therefore be viewed as a localized level to band transition. Higher energy optical interband transitions from the anion p states to the conduction band might be useful to reveal where the conduction band minimum really occurs. Another difference noted between the two cases is that in GdN the spin-polarization induced by the interaction with 4f electrons is reversed for the anion p valence band and the Gd 5d conduction band, whereas in Eu chalcogenides the spin ordering is normal

for both anion p valence and Eu 5d and 6s conduction bands. Thus little spin-polarization is expected for corresponding optical transitions between them.

The total energy differences were calculated between three antiferromagnetic configurations and the ferromagnetic one. We found ferromagnetic ordering to be the ground state for EuO but the antiferromagnetic ordering along {111} to be preferred for EuS, EuSe, and EuTe. This agrees with experiment for EuSe, EuTe, and EuO, but for EuS the actual ground state is believed to be ferromagnetic. We note that some ferromagnetic contribution from carrier mediated interactions cannot be excluded in the experimental samples. In any case, the crossover from ferro-to antiferromagnetic ordering experimentally appears to occur for EuSe rather than for EuS and manifests itself in the occurrence of a complex spiral type ordering.

The energy differences are well accounted for by a Heisenberg Hamiltonian with $S = \frac{7}{2}$ and with nearest- and second-nearest-neighbour interactions. We extracted the values of the exchange interactions J_1 and J_2 from our calculated total energy differences. They agree quite well with the values obtained for EuO and EuS from inelastic neutron scattering measurements of the spin wave excitations by Passell *et al* [55]. They also agree qualitatively with the trends in paramagnetic Curie–Weiss temperatures and critical temperatures T_c or T_N and the exchange parameters that can be extracted from them within mean field theory. It is somewhat surprising that magnetic parameters such as the exchange interactions of order K can be obtained from density functional calculations. It results from a large degree of cancellation of systematic errors in taking the relevant energy differences between magnetic configurations, which are of the order of 10 meV.

Acknowledgments

This work was supported by the Office of Naval Research under grant number N00014-99-1-1073 and the National Science Foundation under grant number ECS-0223634.

References

[1] Wolf S A, Awschalom D D, Buhrman R A, Daughton J M, von Molnar S, Roukes M L, Chtchelkanova A Y and Treger D M 2001 *Science* **294** 1488
[2] Ohno H 1998 *Science* **281** 951
Ohno Y, Young D K, Beschoten B, Ohno H and Awschalom D D 1999 *Nature* **402** 709
Ohno H 2001 *Science* **291** 840
[3] Wachter P 1979 *Handbook on the Physics and Chemistry of Rare Earths* vol 2, ed K A Gschneidner and L Eyring (Amsterdam: Elsevier) p 507
[4] Ghosh D, De M and De S K 2004 *Phys. Rev.* B **70** 115211
[5] Santos T S and Moodera J S 2004 *Phys. Rev.* B **69** 241203
[6] Snow C S, Cooper S L, Young D P, Fisk Z, Comment A and Ansermet J-P 2001 *Phys. Rev.* B **64** 174412
[7] Steeneken P G, Tjeng L H, Elfimov I, Sawatzky G A, Ghiringhelli G, Brookes N B and Huang D-J 2002 *Phys. Rev. Lett.* **88** 047201
[8] Torrance J B, Shafer M W and McGuire T R 1972 *Phys. Rev. Lett.* **29** 1168
[9] Schoenes J and Wachter P 1974 *Phys. Rev.* B **9** 3097
[10] Kunes J and Pickett W E 2005 *Physica* B **359–361** 205
[11] Horne M, Strange P, Temmerman W M, Szotek Z, Svane A and Winter H 2004 *J. Phys.: Condens. Matter* **16** 5061
[12] Sinjukow P and Nolting W 2003 *Phys. Rev.* B **68** 125107
[13] Cho S J 1970 *Phys. Rev.* B **1** 4589
[14] Hulliger F 1979 Rare earth pnictides *Handbook on the Physics and Chemistry of Rare Earths* vol 4, ed K A Gschneider Jr and L Eyring (New York: North-Holland Physics Publishing) pp 153–236
[15] Wachter P and Kaldis E 1980 *Solid State Commun.* **34** 241

[16] Li D X, Haga Y, Shida H and Suzuki T 1994 *Physica* B **199/200** 631
[17] Kasuya T and Li D X 1997 *J. Magn. Magn. Mater.* **167** L1–6
[18] Xiao J Q and Chen C L 1996 *Phys. Rev. Lett.* **76** 1727
[19] Leuenberger F, Parge A, Felsch W, Fauth K and Hessler M 2005 *Phys. Rev.* B **72** 014427
[20] Granville S, Ruck B J, Budde F, Koo A, Pringle D J, Kuchler F, Preston A R H, Housden D H, Lund N, Bittar A, Williams G V M and Trodahl H J 2006 *Phys. Rev.* B at press
[21] Lambrecht W R L 2000 *Phys. Rev.* B **62** 13538
[22] Larson P and Lambrecht W R L 2006 *Phys. Rev.* B **74** 085108
[23] Aerts C M, Strange P, Horne M, Temmerman W M, Szotek Z and Svane A 2004 *Phys. Rev.* B **69** 045115
[24] Duan C-G, Sabiryanov R F, Liu J, Mei W N, Dowben P A and Hardy J R 2005 *Phys. Rev. Lett.* **94** 237201
[25] Schmidt G, Ferrand D, Molenkamp L W, Filip A T and van Wees B J 2000 *Phys. Rev.* B **62** R4790
[26] Lie D X, Haga Y, Shida H, Suzuki T and Kwon Y S 1996 *Phys. Rev.* B **54** 10483
[27] Lie D X, Haga Y, Shida H and Suzuki T 1994 *Physica* B **199/200** 631
[28] Yamada H, Fukawa T, Muro T, Tanaka Y, Imada S, Suga S, Li D-X and Suzuki T 1996 *J. Phys. Soc. Japan* **65** 1000
[29] Jaya S M and Nolting W 1997 *J. Phys.: Condens. Matter* **9** 10439
[30] McGuire T R, Argyle B E, Shafer M W and Smart J S 1963 *J. Appl. Phys.* **34** 1345
McGuire T R, Argyle B E, Shafer M W and Smart J S 1964 *J. Appl. Phys.* **35** 984
[31] Enz U, Fast J F, Van Houten S and Smit J 1962 *Philips Res. Rep.* **17** 451
[32] Busch G, Natterer B and Neukomm H R 1966 *Phys. Lett.* **23** 190
[33] Dimmock J O 1970 *IBM J. Res. Dev.* **14** 301 and references cited therein
[34] Borstel G, Borgiel W and Nolting W 1987 *Phys. Rev.* B **36** 5301
[35] Muller C, Lippitz H, Paggel J J and Fumagalli P 2004 *J. Appl. Phys.* **95** 7172
[36] Kasuya T and Yanase A 1968 *Rev. Mod. Phys.* **40** 684
[37] Hohenberg P and Kohn W 1964 *Phys. Rev.* **136** B864
Kohn W and Sham L J 1965 *Phys. Rev.* **140** A1133
[38] Methfessel M, van Schilfgaarde M and Casali R A 2000 *Electronic Structure and Physical Properties of Solids, The Uses of the LMTO Method (Workshop Mont Saint Odille, France, 1998)* (*Springer Lecture Notes*) ed D Hughes (Berlin: Springer) pp 114–47
[39] von Barth U and Hedin L 1972 *J. Phys. C: Solid State Phys.* **5** 2064
[40] Jepsen O and Andersen O K 1971 *Solid State Commun.* **9** 1763
[41] Blöchl P E, Jepsen O and Andersen O K 1994 *Phys. Rev.* B **49** 16223
[42] Anisimov V I, Zaanen J and Andersen O K 1991 *Phys. Rev.* B **44** 943
Anisimov V I and Gunnarsson O 1991 *Phys. Rev.* B **43** 7570
Anisimov V I, Aryasetiawan F and Liechtenstein A I 1997 *J. Phys.: Condens. Matter* **9** 767
[43] Liechtenstein A I, Anisimov V I and Zaanen J 1995 *Phys. Rev.* B **52** R5467
[44] Dudarev S L, Botton G A, Savrasov S Y, Humphreys C J and Statton A P 1998 *Phys. Rev.* B **57** 1505
[45] Mann J B 1967 Atomic structure calculations I. Hartree–Fock energy results for the elements hydrogen to lawrencium *Los Alamos Internal Report*
[46] Hedin L and Lundqvist S 1969 *Solid State Physics, Advances in Research and Applications* vol 23, ed F Seitz, D Turnbull and H Ehrenriech (New York: Academic) p 1
[47] Hybertsen M S and Louie S G 1985 *Phys. Rev. Lett.* **55** 1418
[48] Godby R W, Schlüter M and Sham L J 1986 *Phys. Rev. Lett.* **56** 2415
[49] Aryasetiawan F and Gunnarsson O 1998 *Rep. Prog. Phys.* **61** 237
[50] Kotani T, van Schilfgaarde M and Faleev S 2005 *Preprint* cond-mat/0510408
[51] Oliver M R, Dimmock J O, McWhorter A L and Reed T B 1972 *Phys. Rev.* B **5** 1078
[52] Yosida K 1996 *Theory of Magnetism* (*Springer Series in Solid State Sciences* vol 122) (Berlin: Springer) chapter 6
[53] Smart J S 1966 *Effective Field Theories of Magnetism* (Philadelphia, PA: W.B. Saunders Company) pp 76–7
[54] Petukhov A G, Lambrecht W R L and Segall B 1996 *Phys. Rev.* B **53** 4324
[55] Passell L, Dietrich O W and Als-Nielsen J 1976 *Phys. Rev.* B **14** 4897